

Charge localization in Co-doped ceria with oxygen vacancies

G.E. Murgida^{a,b,c,*}, V. Vildosola^{a,b}, V. Ferrari^{a,b}, A.M. Llois^{a,b,c}

^a Centro Atómico Constituyentes, GlyA, CNEA, San Martín, Buenos Aires, Argentina

^b Consejo Nacional de Investigaciones Científicas y Técnicas, C1033AAJ, Buenos Aires, Argentina

^c Departamento de Física Juan José Giambiagi, FCEyN, UBA, Buenos Aires, Argentina

ARTICLE INFO

Article history:

Received 24 May 2011

Received in revised form

5 October 2011

Accepted 7 December 2011

by S. Scandolo

Available online 13 December 2011

Keywords:

A. Diluted magnetic oxides

A. Ceria

D. Charge localization

ABSTRACT

In this paper we report density functional theory (DFT) calculations on bulk cerium oxide (ceria) doped with magnetic impurities of cobalt atoms in the presence of oxygen vacancies. Using the framework of the DFT + *U* approach to take into account the effects of electronic correlations in the Ce 4f states, we evaluate the relative stability of different configurations of vacancies. We show that, within the approximations considered, the vacancies tend to locate close to the Co impurities. In addition, we address the issue of the charge localization that takes place due to de-oxygenation processes, finding that the excess electrons reside at Ce atoms which are next-nearest neighbors of the vacancy sites.

© 2011 Elsevier Ltd. All rights reserved.

1. Introduction

In recent years, cerium oxide (ceria) has been subject of intense work in two diverse yet related areas of condensed matter research with the driving force of possible technological applications. On the one hand, the key role played by ceria in catalytic applications is well known, and hence it is of the utmost importance to study its capability for oxygen storage as well as the possibility of reversible oxygen release (see [1] and references therein). On the other hand, the search for and development of novel materials that are ferromagnetic beyond room temperature is also currently being explored for spintronic applications. In this context, ceria with diluted magnetic impurities is a natural candidate, due to its good integrability with current electronic devices. However, this material still poses several questions, the main one being the need to find a widely acceptable explanation for the observed room-temperature ferromagnetism (RTFM) [2]. The physical origin of this RTFM is currently a subject of controversy and debate, but there seems to be consensus that oxygen vacancies play a determining role. It is clear, then, that a complete understanding of the physics involved when oxygen vacancies are created is important for both catalysis and spintronics.

When using cobalt as dopant, there is experimental evidence supporting the idea that the excess electrons, left behind by oxygen

vacancies, localize themselves in specific cobalt and cerium atoms, changing their oxidation states ($\text{Co}^{4+} \rightarrow \text{Co}^{2+}$ and $\text{Ce}^{4+} \rightarrow \text{Ce}^{3+}$, respectively) and turning the cerium atoms into magnetic ions. The location of these magnetic Ce atoms (concomitant with the charge localization of the excess electrons) has then a two-fold importance: it will help us to understand the magnetic properties as well as the catalytic processes in ceria-based systems.

From the theoretical point of view, Skorodumova et al. [3] have proposed that, in reduced bulk ceria, charge localization occurs at Ce sites which are in nearest-neighbor (NN) sites of oxygen vacancies within a framework that coined the name standard model (SM). Recently, this SM view has been challenged by calculations in the bulk [4] as well as in the reduced $\text{CeO}_2(111)$ surface [5,6]. These works report that the charge localization occurs at Ce ions which are in next-nearest-neighbor (NNN) sites of the vacancies.

It has recently been stressed that atomic relaxation is crucial to properly account for charge localization processes [5,7]. To the best of our knowledge, the validity of the SM for partially reduced ceria doped with magnetic impurities has not yet been explored. In this work, we tackle this problem by focusing on the location of vacancies along with the charge localization in the corresponding Ce atoms.

2. Structural configurations

We consider CeO_2 supercells with substitutionally doped Co impurities and with oxygen vacancies, assuming that the dopant is homogeneously distributed. To evaluate whether the SM is valid for Co-doped ceria, it is essential to use a supercell with a

* Corresponding author at: Centro Atómico Constituyentes, GlyA, CNEA, San Martín, Buenos Aires, Argentina. Tel.: +54 11 4206 4648.

E-mail addresses: murgida@tandar.cnea.gov.ar, gmurgida@df.uba.ar (G.E. Murgida).

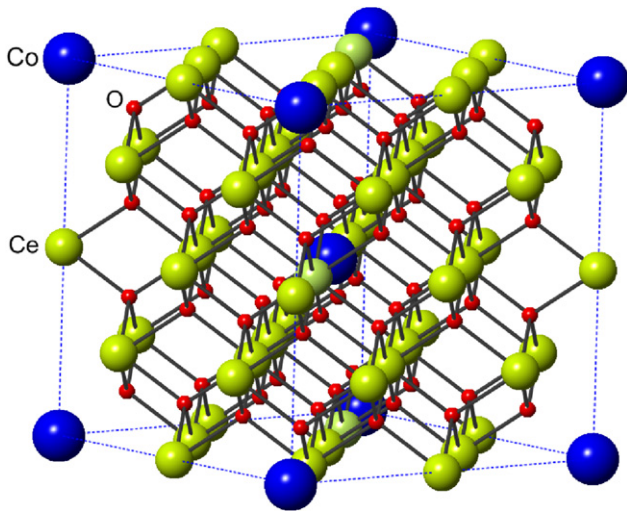


Fig. 1. (Color online) $2 \times 2 \times 2$ BCC-type unit cell corresponding to 6.25% cobalt concentration. O atoms are denoted by small red (dark) balls, Ce ions by big green (light) balls and Co atoms by big blue (dark) balls.

Co concentration that is low enough to accommodate the excess charge into Ce ions located at two possible locations: either at the NN or at the NNN sites with respect to the oxygen vacancies. Therefore we choose a $2 \times 2 \times 2$ body-centered cubic (BCC)-type supercell, corresponding to an atomic Co concentration of 6.25% (see Fig. 1). This doping concentration is well within the range of values reported in the literature for real samples [8].

In this situation, there are four electrons left behind by the oxygen vacancies. As already mentioned, X-ray experiments suggest that in oxygen-deficient samples the valence of Co is 2+ (see [9–11]). We therefore assume that the Co atom is in this valence state and that two electrons should be located at certain Ce sites, with the consequent change of the oxidation state into Ce^{3+} ions. Within these assumptions, the minimal number of vacancies per Co atom to get Ce^{3+} ions is two (namely, 6.25%), as with only one vacancy there are no extra electrons to be localized into Ce sites.

Fig. 2 shows the six calculated configurations for different positions of both oxygen vacancies and the Ce^{3+} sites with respect to the impurity atom. To denote the configurations, we use a notation to describe if the atoms are in either NN or NNN sites (see description in the caption of Fig. 2). Note that only two configurations (i.e. 111 and 211) satisfy the SM, namely the ones where the excess charge gets localized at Ce sites that are NN sites to the vacancies.

3. Computational details

The calculations are performed using self-consistent first-principles density functional theory (DFT) within the local spin density approximation (LSDA) for the exchange–correlation potential as implemented in the ab initio code Wien2k [12]. This code implements the full-potential augmented plane waves method. We use muffin tin (MT) radii values $R_{\text{Ce}}^{\text{MT}} = 2.3$ a.u., $R_{\text{Co}}^{\text{MT}} = 1.9$ a.u., and $R_{\text{O}}^{\text{MT}} = 1.6$ a.u. The number of plane waves in the interstitial region is given by $R^{\text{MT}}K_{\text{max}} = 7$, and we use 200 k -points in the irreducible part of the Brillouin zone.

In order to describe the charge localization on the 4f states occupied in the Ce^{3+} ions, it is necessary to go beyond LSDA to properly account for the local strong Coulomb interaction [13–15]. The structures are first allowed to relax by taking these 4f electrons as core levels, until the forces on the atoms are below 1 mRy/au. This procedure is performed to facilitate symmetry breaking, which

Table 1

ΔE is the total energy per Co atom with respect to E_0 , the lowest-energy configuration, namely $\Delta E = E - E_0$. The configurations are depicted in Fig. 2.

Configuration	111	121	122	211	221	222
ΔE (eV)	0.23	0.14	0	0.23	1.71	1.99

is crucial to effectively localize the 4f electrons. Afterwards, the relaxation is carried out further with the 4f electrons in the valence band and using the LSDA + U approach to switch on the local Coulomb interaction in the Ce^{3+} ions. We take $U_{\text{eff}} = U - J = 6$ eV [14,15]. In order to check the effect of strong correlations in the Co impurity, we have performed calculations with and without a DFT + U treatment in the Co 3d levels.¹ The inclusion of U in the treatment of Co modifies the absolute values of the total energies but not the differences among the considered configurations, which remain invariant. Hereafter, to discuss the effect of charge localization, we present the results obtained without a DFT + U treatment of the Co sites.

4. Oxygen vacancies, charge localization, and relaxation processes

Within the approximations used, we find that the lowest energy configuration is the 122 one, depicted in Fig. 3(c). Table 1 shows the calculated total energy differences with respect to this lowest-energy configuration. In this case, the oxygen vacancies are in NN sites to the Co atom and in NNN sites to the Ce^{3+} site. Therefore, two out of the four extra electrons tend to locate far away from the vacancy sites, in particular in an NNN Ce site. This result indicates that the SM is not the most favourable situation for the present case of reduced Co-doped ceria.

Another important conclusion that can be drawn from this table is that the vacancies prefer to be close to the Co atom. The 221 and 222 configurations, in which the vacancies are located further away from the Co atom, are around 2 eV higher in energy than those where the vacancies are in NN sites of the Co atom. This nucleation capability of the Co impurity has also been obtained even within the SM [7], suggesting that the physical origin of the nucleation might be independent of the charge localization.

The 211 configuration deserves special consideration. Although we started off with this configuration (as depicted in Fig. 2(d)), i.e. with the vacancies located far away from the Co atom, at the end of the relaxation process the structure evolves into a 111-type configuration (see Fig. 3(d)). This atomic rearrangement can also be seen as the oxygen vacancies “moving” to an NN site of the impurity, a fact that is also evident in the value of the total energy, as shown in Table 1.

As mentioned above, the atomic reorganization after the release of oxygen atoms directly affects the physical properties in these systems. On the one hand, the relaxation of the atoms facilitates not only the adjustment of the electronic structure of the charge-receptive Ce atoms [17], but also the reduction process itself, making it more feasible [5]. On the other hand, the magnetic properties are very sensitive to the atomic positions, as relaxation allows for the existence and location of the magnetic Ce^{3+} ions.

To get insight into the physical origin of our results regarding the different configurations for charge localization in Co-doped ceria, we now describe the atomic relaxations for two particular configurations (i.e. 122 and 111). The comparison between them is interesting because the 111 configuration satisfies the SM, while the energetically most favorable one (i.e. 122), does not.

¹ For the DFT + U treatment of the Co 3d levels, we take $U_{\text{eff}} = 5$ eV, which is within the range of values considered in the literature [16].

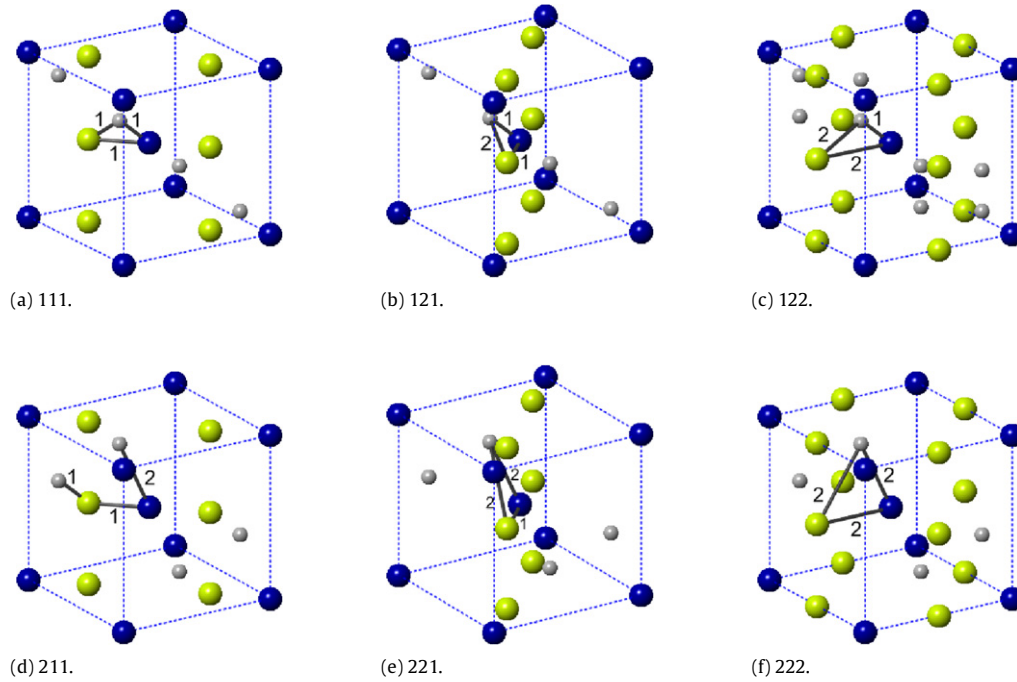


Fig. 2. (Color online) Structural configurations taking into account different positions of the oxygen vacancies (denoted with small gray/bright balls) and Ce^{3+} sites (big green/bright balls) with respect to the Co atom (big blue/dark balls). For simplicity, the other atoms (oxygen and Ce^{4+} atoms) within the supercell are not shown in the picture. The bond sticks labeled as “1” refer to NN sites while sticks labeled as “2” stand for NNN sites. The three-number code denoting each configuration describes the character (either NN or NNN) of the Co–vacancy/Ce–vacancy/Co–Ce distances.

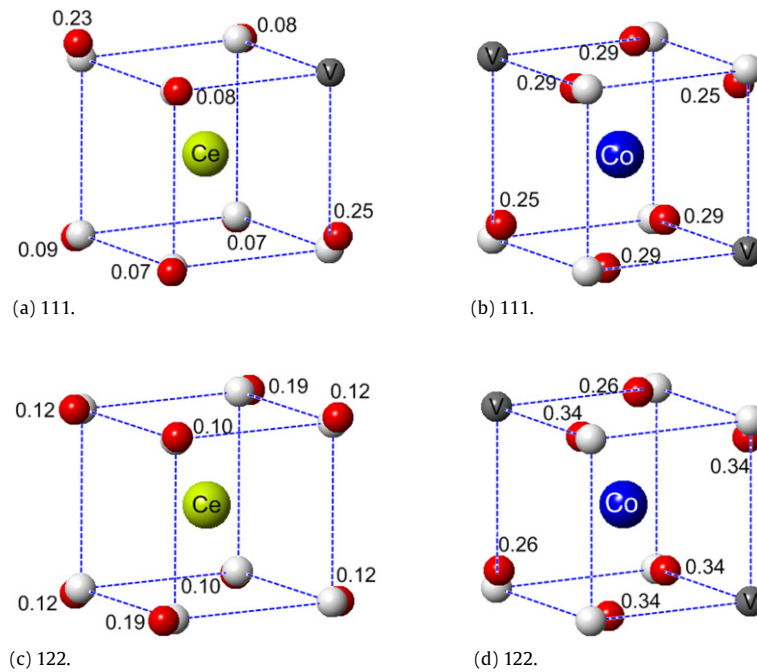


Fig. 3. (Color online) Relaxation of the oxygen atoms surrounding the impurity and the Ce^{3+} for two configurations, namely 111 (a) and (b) and 122 (c) and (d) (see text). The relaxed oxygen positions (small red balls) are superposed to the unrelaxed ones (small bright grey balls). The color coding for the other atoms is the same as in Fig. 2. The numbers indicate the atomic displacement with respect to the unrelaxed position in Å.

Fig. 3 describes the relaxation of the oxygen atoms which are neighbors to the Co impurity and to the Ce^{3+} ions for the 111 and 122 configurations, respectively. This figure shows that during the relaxation process the oxygen atoms move towards both the vacancy sites and the Co atoms, while migrating away from the Ce^{3+} ions. In the lowest-energy configuration, the average Ce^{3+} –O

bond length is 2.44 Å while in the 111 structure it is 2.40 Å. We note that the former value is closer to the Ce–O bond length in Ce_2O_3 (2.50 Å), where all Ce atoms are in the 3+ valence state. This gives some indication about the 122 configuration being more energetically favorable than the 111 configuration. Similar results have been reported in reduced CeO_2 (111) surfaces [5].

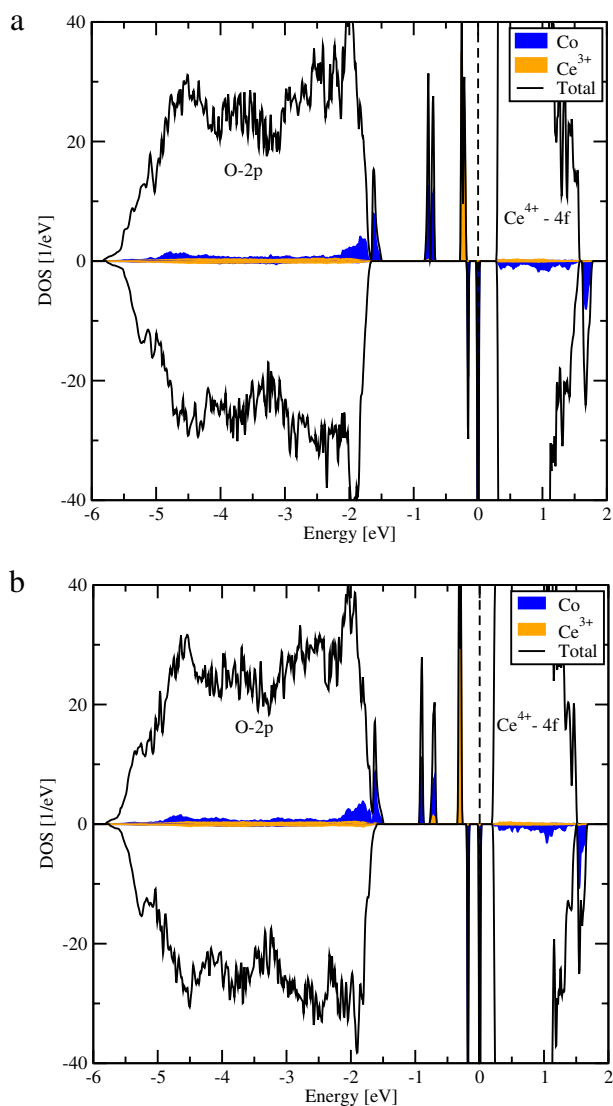


Fig. 4. (Color online) Density of states for Co-doped CeO_2 with oxygen vacancies. (a) 122 configuration and (b) 111 configuration. Total DOS (black line), partial DOS for cobalt (blue) and Ce^{3+} (orange). The minority spin channels are shown inverted.

5. Electronic structure

In Fig. 4, we plot the total densities of states (DOSs) as well as the partial ones for both Co and Ce^{3+} . The occupied bands are mainly of O 2p character and the unoccupied ones are mostly Ce 4f. Within the gap, several sharp peaks appear, when oxygen vacancies are formed, due to the presence of Co impurities and Ce^{3+} ions. The presence of the Ce^{3+} peak is the signature that the charge left behind by the oxygen vacancies is localized at a particular Ce site as a $4f^1$ state. There is also some band hybridization of both Co and Ce states with the O 2p ones. The above description applies qualitatively for 122 configuration as well as for the 111 configuration (Fig. 4(a) and (b), respectively). The main difference between them is that two of the majority impurity peaks are further apart in energy in the 111 configuration than in the 122 one. The relative shifts of the impurity peaks might be understood by taking into account that there is a stronger hybridization between the Co and the Ce^{3+} peaks in the 111 configuration. This

hybridization is, in turn, a consequence of the Co and Ce^{3+} ions being closer in the 111 configuration compared to the 122 one.

6. Discussion and conclusions

We have evaluated the relative stability for different configurations of oxygen vacancies and charge localization in Co-doped ceria within the framework of the LSDA + U approach. We found that oxygen vacancies lying close to the Co impurities renders the lowest-energy situation. Regarding charge localization, we have demonstrated that the excess electrons due to a de-oxygenation process reside at those Ce ions which are NNN sites of the vacancies. This configuration, in turn, allows Ce^{3+} ions to get nearer to their usual ionic volume. Summarizing, from the energetic point of view, the SM is not the most favorable configuration for the present case of reduced Co-doped ceria. Our results are consistent with previous ab initio studies for reduced $\text{CeO}_2(111)$ surfaces [5] where charge localization also occurs at NNN sites of the vacancies.

Acknowledgments

The authors acknowledge the financial support from ANPCyT, CONICET and UBA for the following grants: PICT-R1776, PIP-0258, PIP-0038, and UBACyT-X123. V.F., V.L., and A.M.L. belong to CONICET's research staff.

References

- [1] F. Esch, S. Fabris, L. Zhou, T. Montini, C. Africh, P. Fornasiero, G. Comelli, R. Rosei, *Science* 309 (2005) 752.
- [2] K. Sato, L. Bergqvist, J. Kudrnovsk, P.H. Dederichs, O. Eriksson, I. Turek, B. Sanyal, G. Bouzerar, H. Katayama-Yoshida, V.A. Dinh, T. Fukushima, H. Kizaki, R. Zeller, *Rev. Modern Phys.* 82 (2010) 1633.
- [3] N.V. Skorodumova, S.I. Simak, B.I. Lundqvist, I.A. Abrikosov, B. Johansson, *Phys. Rev. Lett.* 89 (2002) 166601.
- [4] E. Shoko, M.F. Smith, R.H. McKenzie, *J. Phys.: Condens. Matter* 22 (2010) 223201.
- [5] M.V. Ganduglia-Pirovano, J.L.F. DaSilva, J. Sauer, *Phys. Rev. Lett.* 102 (2009) 026101.
- [6] H. Li, H. Wang, X. Gong, Y. Guo, Y. Guo, G. Lu, P. Hu, *Phys. Rev. B* 79 (2009) 193401.
- [7] V. Ferrari, A.M. Llois, V. Vildosola, *J. Phys.: Condens. Matter* 22 (2010) 276002.
- [8] A. Tiwari, V.M. Bhosle, S. Ramachandran, N. Sudhakar, J. Narayan, S. Budak, A. Gupta, *Appl. Phys. Lett.* 88 (2006) 142511; Y. Song, H. Zhang, Q. Wen, H. Zhu, J. Xiao, *J. Appl. Phys.* 102 (2007) 043912; Q. Wen, H. Zhang, Y. Song, Q. Yang, H. Zhu, J. Xiao, *J. Phys.: Condens. Matter* 19 (2007) 246205; L. Bi, H. Kim, G.F. Dionne, S.A. Speakman, D. Bono, C.A. Ross, *J. Appl. Phys.* 103 (2008) 07D138.
- [9] B. Vodungbo, F. Vidal, Y. Zheng, M. Marangolo, D. Demaille, V.H. Etgens, J. Varalda, A.J.A. de Oliveira, F. Maccherozzi, G. Panaccione, *J. Phys.: Condens. Matter* 20 (2008) 125222. 10.
- [10] Y. Song, H. Zhang, Q. Wen, L. Peng, J. Xiao, *J. Phys.: Condens. Matter* 20 (25) (2008) 255210.
- [11] Q. Wen, H. Zhang, Y. Song, Q. Yang, H. Zhu, J. Xiao, *J. Phys.: Condens. Matter* 19 (24) (2007) 246205.
- [12] P. Blaha, K. Schwarz, G. Madsen, D. Kvasnicka, J. Luitz, WIEN2k, An augmented Plane Wave + local orbitals program for calculating crystal properties, Techn. Universität Wien, Austria, SBN 3-9501031-1-2, 2002.
- [13] M.V. Ganduglia-Pirovano, A. Hofmann, J. Sauer, *Surf. Sci. Rep.* 62 (2007) 219. and references therein.
- [14] C.W.M. Castleton, J. Kullgren, K. Hermansson, *J. Chem. Phys.* 127 (2007) 244704.
- [15] D.A. Andersson, S.I. Simak, B. Johansson, I.A. Abrikosov, N.V. Skorodumova, *Phys. Rev. B* 75 (2007) 035109.
- [16] V.I. Anisimov, J. Zaenon, O.K. Andersen, *Phys. Rev. B* 44 (1991) 943; L. Wang, T. Maxisch, G. Ceder, *Phys. Rev. B* 73 (2006) 195107; X. Wang, M. Shen, J. Wang, S. Fabris, *J. Phys. Chem. C* 114 (2010) 10221.
- [17] Without a proper atomic relaxation, the $\text{Ce}^{4+} \rightarrow \text{Ce}^{3+}$ reduction process cannot be achieved.